Proceedings of the National Academy of Sciences
Vol. 67, No. 1, pp. 213–220, September 1970

The Septate Junction: A Structural Basis for Intercellular Coupling*

Norton B. Gilula†, Daniel Branton‡, and Peter Satir†

DEPARTMENTS OF PHYSIOLOGY-ANATOMY† AND BOTANY‡, UNIVERSITY OF CALIFORNIA, BERKELEY, CALIF. 94720

Communicated by H. A. Barker, June 22, 1970

Abstract. Electron microscopy, freeze-etching, and optical diffraction show how the structure of the septate junction may provide the basis for the low-resistance pathway between the electrically coupled cells in mussel gill epithelia. Conventional electron microscopy suggests that the septa are pleated sheets that differentiate from and are structurally continuous with the junctional cell membranes. Freeze-etching exposes geometrically arranged rows of 85-Å particles within the junctional cell membranes. Diffraction evidence shows that these membrane particles and the alternate vertices of the intercellular septal sheets are congruent and therefore superposable. Together, the membrane particles and septal sheets provide a channel that extends from the cytoplasm of one cell through the septate junction to the cytoplasm of the adjacent cell.

Electrophysiological evidence has established that many cells are coupled to one another across their boundaries.[1–4] This coupling has been attributed to morphologically unique junctions between adjacent cell membranes: the gap junction found in nerve[5–7], epithelium[8], and muscle tissue[9,10]; and the septate junction (originally termed septate desmosome)[11] of invertebrate epithelia.[12,13]

At the apical regions of the ciliated lateral cells in mussel gill filaments, the septate junction is a belt-like structure 2–3 μm wide. The cell membranes of the junction are separated by a 150 Å intercellular space which is regularly traversed by septa that join the membranes of the two cells. It has been suggested that the septate junction could function in intercellular adherence,[11] as an occluding barrier,[11] or, according to the most recent evidence, as a coupling structure.[13,14] The investigation described here utilizes conventional electron microscopy, freeze-etching, and optical diffraction evidence to show how the structure of the septate junction may account for its coupling function.

Materials and Methods. Intact gills of freshwater mussels, mainly *Elliptio complanatus*, were excised and cut into small (2 mm) pieces.

For positive staining, the tissue was fixed for 2–4 hr at room temperature in 0.1 M cacodylate-buffered 5% glutaraldehyde (pH 7.3) and postfixed for 1 hr at room temperature in 0.1 M cacodylate-buffered 1% osmium tetroxide (pH 7.3). Alternatively, osmium post-fixation was replaced by uranyl acetate block staining.[15] Ruthenium red staining was according to Luft.[16] All materials were dehydrated in an ethanol series plus propylene oxide, and embedded in Epon 812. Thin sections were obtained with a Porter-Blum MT-2 ultramicrotome and usually post-stained with magnesium uranyl acetate and lead citrate before examination in a Siemens Elmiskop 1A at 80 kV.

For freeze-etching, small pieces of the gill tissue were fixed for 15–30 min in cacodylate-buffered 2.5% glutaraldehyde and then soaked in 30% glycerol for 2–6 hr. Pieces of the tissue were mounted on 3 mm cardboard disks and frozen rapidly in liquid Freon 22. All of the tissue was freeze-etched in a Balzers apparatus using 1 min of etching at −100°C.[17,18] The shadowed direction is from bottom to top on all micrographs, and shadows are white.

Diffraction patterns of suitably reduced electron micrographs were obtained using an Electro-Optics 0.5 mW He–Ne Gas Laser.

Results. Conventional electron microscopy: The positively stained image of the septate junction (Figs. 1 and 2) shows the septa and the two outer leaflets of the 80 Å unit membranes as electron-dense. The septal size is nearly constant, but the interseptal space varies from 50 to 140 Å (compare Figs. 1 and 2). Tangential views show a series of parallel pleated or corrugated sheets with a hexagonal substructure in some regions (Fig. 5b).

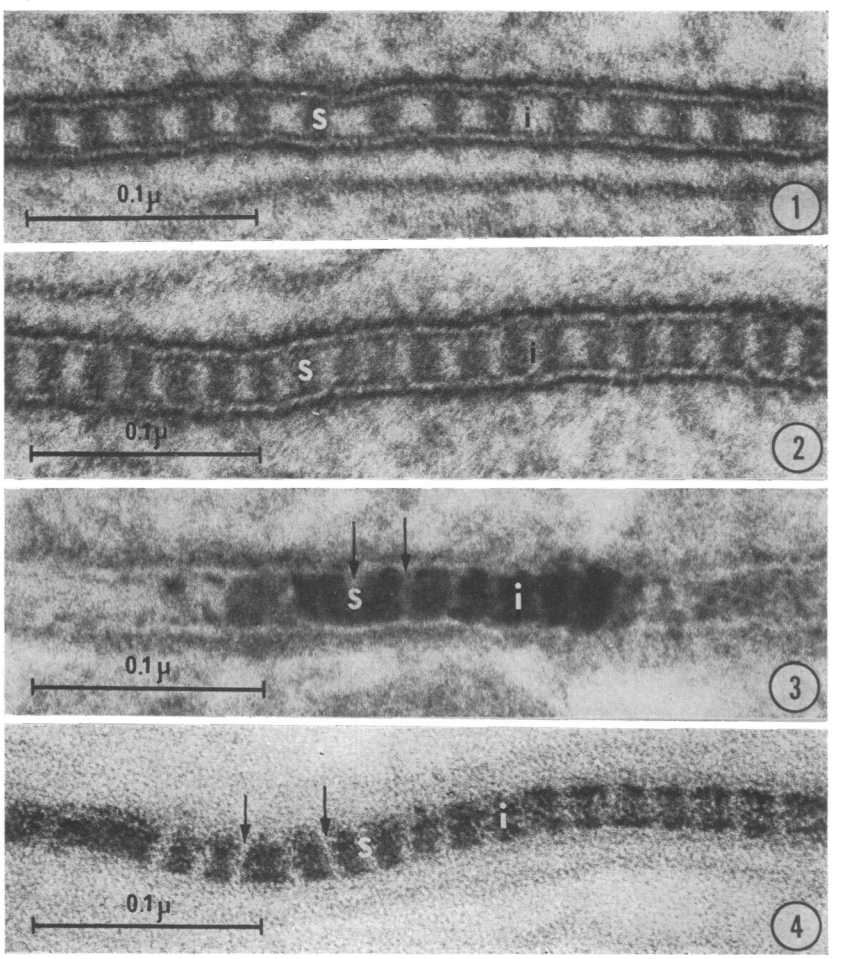

FIGS. 1–4. Cross sections of the septate junction. FIGS. 1–2: Conventional appearance after positive staining. FIGS. 3–4. Negative appearance after uranyl (Fig. 3) or ruthenium red (Fig. 4) block treatment. Ruthenium red localizes acid mucopolysaccharides in the interseptal space (*i*). Arrows indicate confluence of septa (*s*) and cell membranes. All ×300,000.

Sections from preparations block stained with uranyl acetate (Fig. 3) show the junction in negative contrast. The unit membranes and the septa are electron-transparent, while the interseptal space is electron-dense. The septa are less than 50 Å wide and are continuous with the surfaces of both cell membranes. Tangential views show the array of pleated sheets in negative contrast (Fig. 5*a*). These pleated sheets are 40–50 Å wide, and their vertices are related to each other as the corners of a hexagon with 124-Å sides (Figs. 5*c* and 6).

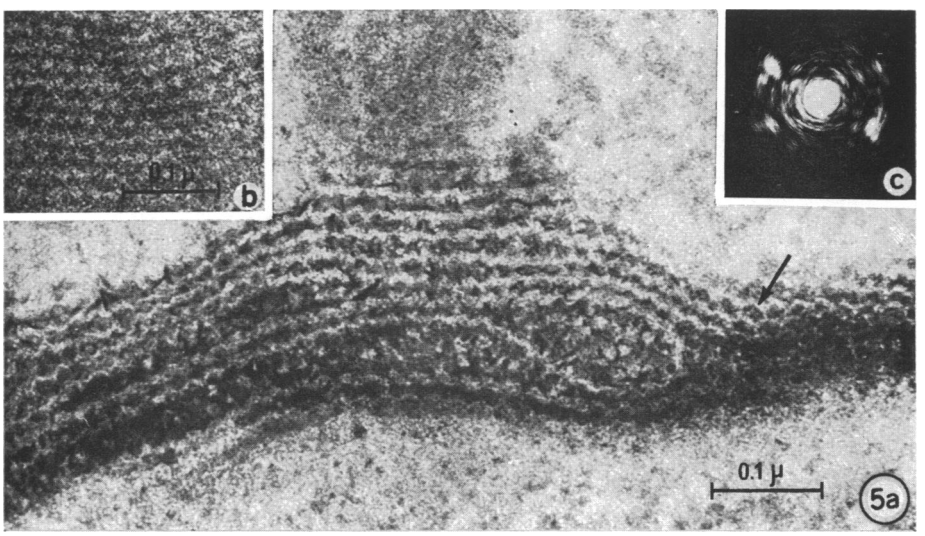

FIG. 5. Thin sections and optical diffraction patterns of tangential views of the septate junction. Both the uranyl block staining (*a*, × 140,000) and the positive staining (*b*, ×120,000) demonstrate arrays of pleated septal sheets which outline hexagons (arrow). (*c*) Optical diffraction pattern of image in 5a shows an incomplete hexagon (see Fig. 6).

After treatment with ruthenium red, the septa are electron-transparent, while the interseptal material becomes electron-dense (Fig. 4). This image corresponds in all important respects to the negative contrast image obtained with uranyl acetate block staining. Ruthenium red stains all of the cell coat material in the junctional regions and on the apical cell surfaces, but it does not stain the septa.

Fig. 6 is a three-dimensional model that reconciles the positive and negative contrast images of the septate junction. The septa are in reality pleated sheets. Since thin sections are about 500 Å thick, in a positive contrast cross section a 50-Å thick sheet would, because of its pleats, appear as a dark septum 80–110 Å thick. In a negative contrast cross section, a 50-Å pleated sheet would appear as a light septum less than 50 Å thick because the dense stain of the interseptal material reverses the section thickness effect.

Freeze-etching: The septate junctional region shows two fracture faces arbitrarily labeled A and B (Figs. 7 and 8). Face A, adjacent to the intercellular space, possesses fewer particles than face B which is adjacent to the cytoplasm. The particles on face B are about 85 Å in diameter, and, as the cross fractures

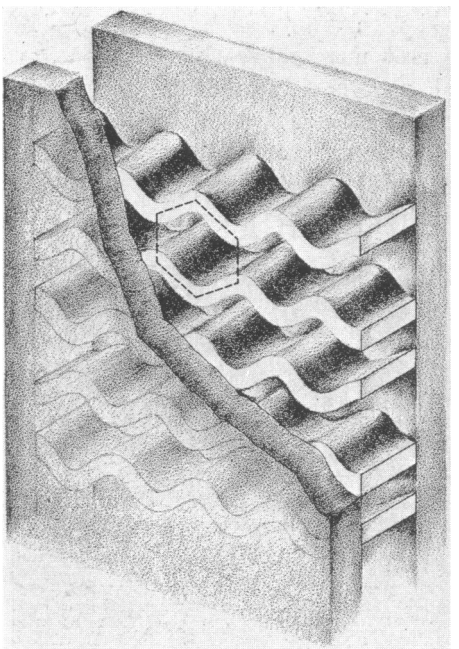

FIG. 6. Model of the septate junction based on conventional electron microscopy. The pleated sheets may form a complete hexagon (*dashed lines*) where they come into contact with the cell membranes.[36]

show, they occur in rows in line with the septa. Extended face views of the septate junction (Fig. 9*a*) show that the two fracture faces A and B are complementary. The face A rows of depressions appear to be continuous with the particle rows found on face B. In regions of the cell where there is no septate junction, face B has fewer particles, and they are not arranged in rows (Fig. 8, *X*).

Optical diffraction: The spacing between rows of particles or depressions is variable, but the packing of both particles and depressions is frequently hexagonal (Fig. 9*b–d*). The pattern from face A yields a hexagon with 124-Å sides (Fig. 9*c*). A congruent hexagon is obtained from diffraction patterns of the negative contrast images (Fig. 5*c*), while the hexagon from face B has a larger side of 210 Å (Fig. 9*d*).

Discussion. The relation between the junctional pleated sheets seen in stained preparations and the particles exposed in freeze-etched material is interpreted in Fig. 10. This model postulates that the particles are located within the membranes at the alternate vertices of the pleated sheets, providing the basis for a structural pathway that appears to be responsible for the coupling between these cells.

We postulate that the particles are located within the junctional membranes because macromolecular labeling experiments have produced compelling evidence that the morphological features of membrane surfaces are not exposed by the fracture process of freeze-etching.[19,20] The fracture process exposes, instead, internal features that are buried within the hydrophobic matrix of the membrane. Similar conclusions have been derived from fractures of frozen isotope-labeled synthetic lipid membranes[21] and freeze-etched preparations of many biological membranes.[18,22–25] In all of these cases the membranes appear to have but one unique fracture plane.[26] Fracturing splits the membrane to expose two inner membrane faces.

We also postulate a congruence between the distribution of the junctional membrane particles and the alternate vertices of the pleated sheets because of several lines of evidence. (1) The particles are continuous with the septa (Figs. 7 and 8). (2) Extended face views (Fig. 9*a*) can best be interpreted as revealing a complementarity between the face A rows of depressions and face B rows of particles. Since this complementarity extends across the 150 Å intercellular

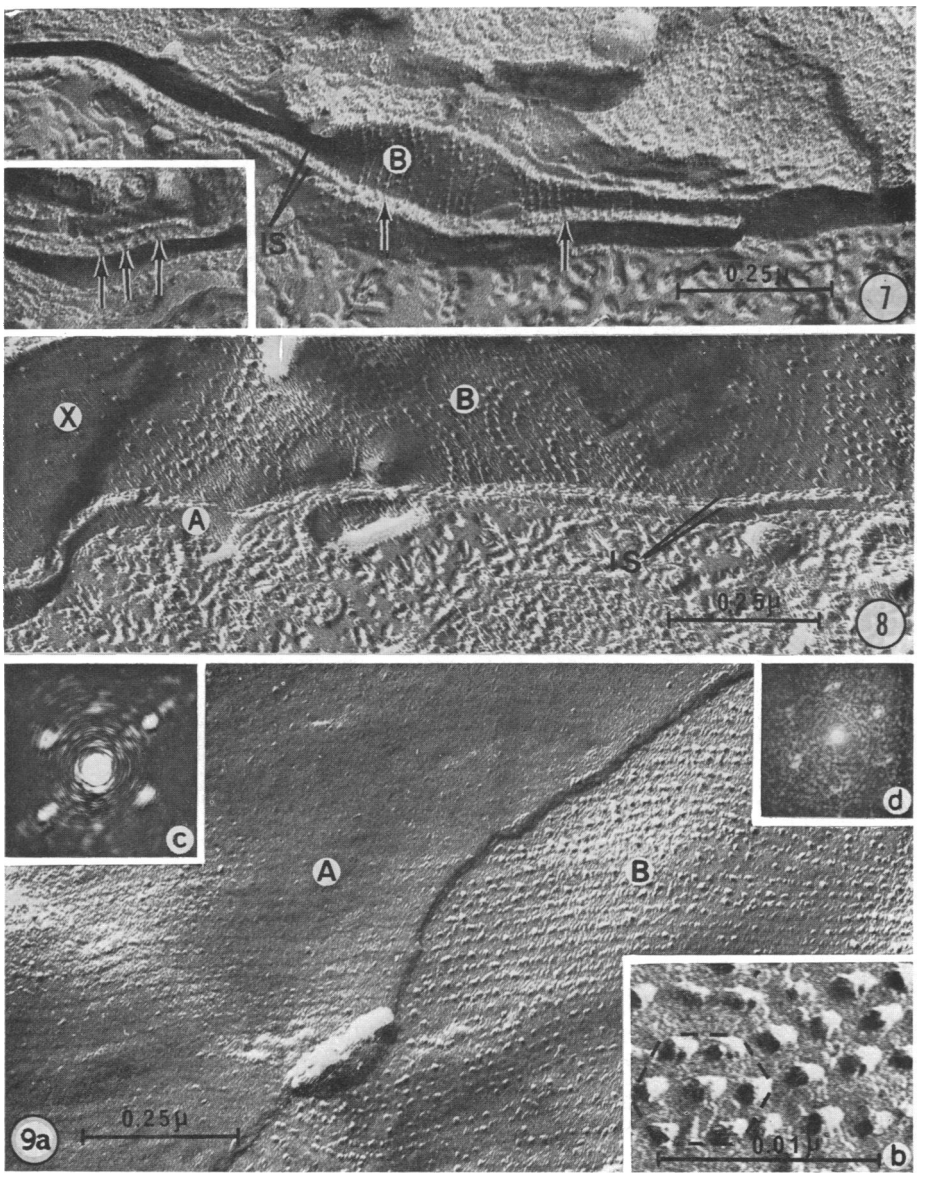

FIGS. 7–8. Freeze-etch images of cross fractures through the septate junctional region showing the intercellular space (*is*), the septa (*arrows*), the membrane face (*B*) with rows of 85 Å particles continuous with the septa, the nonparticle face (*A*), and a nonjunctional region of the cell membrane (*X*). Both ×80,000.

FIG. 9. (*a*) Tangential fracture through the junctional membranes. The rows of depressions on the nonparticle face (*A*) complement the rows of particles on face *B*. ×80,000. (*b*) The particles in face *B* frequently display hexagonal packing. ×288,000. (*c–d*) Optical diffraction pattern from face *A* image (*c*) and face *B* image (*d*).

space, the intercellular septa must act as matchmakers. (3) Congruent hexagons with 124 Å sides are obtained from diffraction patterns of face A (Fig. 9*a*) and of negative contrast images of the pleated sheets (Fig. 5*a*). Therefore,

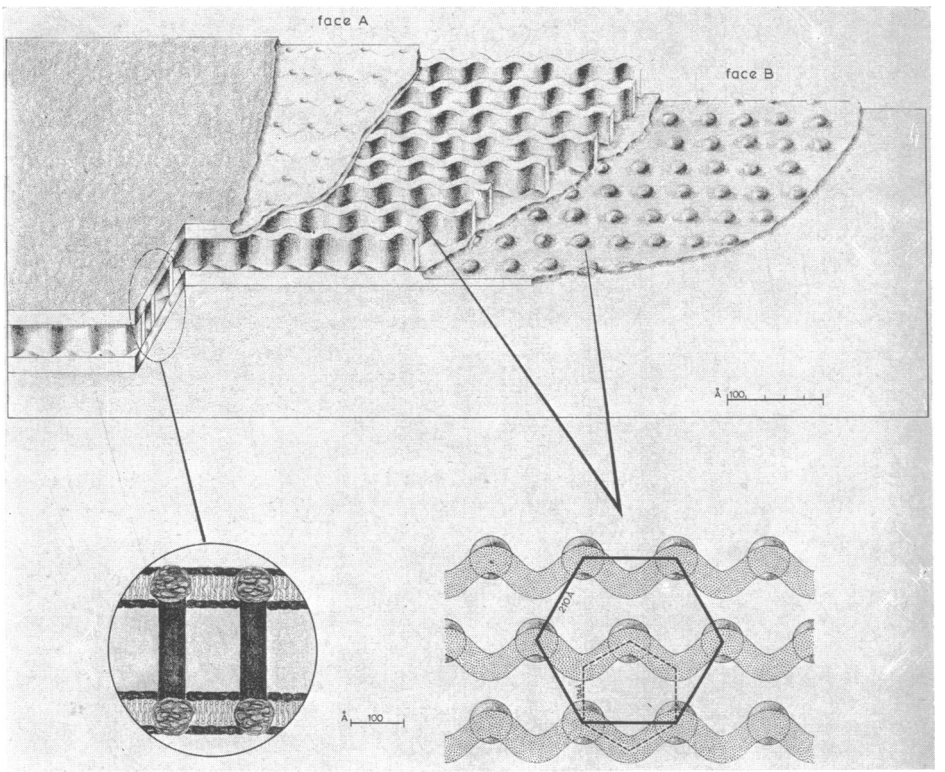

FIG. 10. Diagrammatic representation of the septate junction. We postulate (lower left) that the low-resistance pathway is a result of a continuity between the particles within the membranes and the intercellular septa.

the face A arrangements and the pleated sheets can be superposed, and the depressions in face A can be considered an expression of the continuity of the septa. (4) The regular hexagon obtained from the diffraction pattern of face B has a 210-Å side, which is much larger than the other arrays. The larger array from face B is accounted for geometrically by placing the particles at alternating vertices of the pleated sheets (Fig. 10, lower right).

A low-resistance pathway is probably formed by the continuity of membrane particles and septal sheets. Work with a variety of other systems suggests that the particles represent modifications or interruptions in a membrane with a lipid bilayer continuum.[19,22,25] These modifications may represent localized proteinaceous intercalations[19,27,28] whose electrical resistance would be considerably lower than that of a simple lipid bilayer.

The septa, rather than the interseptal space as previously postulated,[13] are the extracellular portions of the pathway. Our recent experiments using pyroantimonate[29,30] support this interpretation. Pyroantimonate precipitates cations[31] and in our junction was periodically localized opposite the septa.[30] A 20–25 Å channel, which may be postulated on physiological grounds,[1,2] would easily fit within the 50-Å thick septum to allow the movement of most ionic species and other small molecules.

We have no evidence at this time for two features of the model: (1) the extent to which the 85-Å particles traverse the membrane; and (2) the manner in which the particles and the septa are joined.

Images of the septa after uranyl block staining or after ruthenium red staining (Figs. 3 and 4) show that the septal material is continuous with the junctional membranes. Ruthenium red, which is known to stain acid mucopolysaccharides, stains only the interseptal space and the cell coat but not the septa, which must be chemically different. This result, along with the observation that portions of the septa remain attached to the junctional membranes when they are pulled apart,[29,32] strongly suggests that the septa are indeed products of the junctional membranes and not products arising from differentiation of the intercellular material. If this is the case, the entire structural pathway is a product of the junctional membrane.[33]

Fractures such as the one in Fig. 8 have enabled us to examine the cell-membrane structure from the apical border to the basal lamina. The septate junction is the only specialized structure that has been found which could be responsible for the known coupling between cells in this tissue.[29] The variability of the interseptal space could control junctional activity: decreasing or increasing the interseptal space would, in turn, increase or decrease the density of permeability sites within the junction. Different types of septate junctional morphology (lamellar and comb) have been reported;[34] however, these morphological variations must have a very minor effect, if any, on the physiological role of the septate junction.

Gap and septate junctions have similar hexagonal arrangements of particles within their membranes.[35] The fact that a similar arrangement occurs in both of these highly specialized junctional membranes suggests that this arrangement has important functional attributes. Our diffraction evidence shows that the membrane particles may be superposed on the alternate vertices of the septal pleated sheets to provide the structural basis for the low-resistance pathway between the electrically coupled cells. Future work must demonstrate the dependence of coupling on the integrity of the structural pathway and ascertain the biochemical nature of the structural modifications.

We thank R. Glaeser for the use of his diffractometer, Eleanor Crump for her help preparing the manuscript, Marjorie Smith for the drawings, and the staff of the Electron Microscope Laboratory.

* Supported by USPHS GM 15859, AMA-ERF, and AEC Contract AT (04-3)-34, P.A. 142. Dr. Gilula was a Public Health Service predoctoral trainee.

[1] Loewenstein, W. R., *Ann. N. Y. Acad. Sci.*, **137**, 441 (1966).
[2] Furshpan, E. J., and D. D. Potter, in *Current Topics in Developmental Biology*, eds. A. Moscona and A. Monroy (New York: Academic Press, 1968), **3**, 95.
[3] Bennett, M. V. L., *Ann. N. Y. Acad. Sci.*, **137**, 509 (1966).
[4] Sheridan, J. D., *J. Cell. Biol.*, **37**, 650 (1968).
[5] Robertson, J. D., *J. Cell Biol.*, **19**, 201 (1963).
[6] Pappas, G. D., and M. V. L. Bennett, *Ann. N. Y. Acad. Sci.*, **137**, 495 (1966).
[7] Payton, B. W., M. V. L. Bennett, and G. D. Pappas, *Science*, **166**, 1641 (1969).
[8] Brightman, M. W., and T. S. Reese, *J. Cell Biol.*, **40**, 648 (1969).
[9] Revel, J. P., and M. J. Karnovsky, *J. Cell Biol.*, **33**, C7 (1967).
[10] Dewey, M. M., and L. Barr, *J. Cell Biol.*, **23**, 553 (1964).

[11] Wood, R. L., *J. Biophys. Biochem. Cytol.*, **6**, 343 (1959).
[12] Wiener, J., D. Spiro, and W. R. Loewenstein, *J. Cell Biol.*, **22**, 587 (1964).
[13] Bullivant, S., and W. R. Loewenstein, *J. Cell Biol.*, **37**, 621 (1968).
[14] Loewenstein, W. R., and Y. Kanno, *J. Cell Biol.*, **22**, 565 (1964).
[15] Kellenberger, E., A. Ryter, and J. Sechaud, *J. Biophys. Biochem. Cytol.*, **4**, 671 (1958).
[16] Luft, J. H., *J. Cell Biol.*, **23**, 54A (1964).
[17] Moor, H., and K. Muhlethaler, *J. Cell Biol.*, **17**, 609 (1963).
[18] Branton, D., *Proc. Nat. Acad. Sci. USA*, **55**, 1048 (1966).
[19] Pinto da Silva, P., and D. Branton, *J. Cell Biol.*, **45**, 598 (1970).
[20] Tillack, T. W., and V. T. Marchesi, *J. Cell Biol.*, **45**, 649 (1970).
[21] Deamer, D. W., and D. Branton, *Science*, **158**, 655 (1967).
[22] Branton, D., *Ann. Rev. Plant Physiol.*, **20**, 209 (1969).
[23] Meyer, H. W., and H. Winkelmann, *Protoplasma*, **68**, 253 (1969).
[24] Branton, D., and R. B. Park, *J. Ultrastruct. Res.*, **19**, 283 (1967).
[25] Branton, D., *Exp. Cell Res.*, **45**, 703 (1967).
[26] Wehrli, E., K. Muhlethaler, and H. Moor, *Exp. Cell Res.*, **59**, 336 (1970).
[27] Branton, D., *Proc. Roy. Soc. Ser. B*, in press.
[28] Glazer, M., H. Simpkins, S. J. Singer, M. Sheetz, and S. I. Chan, *Proc. Nat. Acad. Sci. USA*, **65**, 721 (1970).
[29] Gilula, N. B., and P. Satir, *J. Cell Biol.*, **43**, 43a (1969).
[30] Satir, P., and N B. Gilula, *J. Cell Biol.*, in press.
[31] Tandler, C. J., C. M. Libanati, and C. A. Sanchis, *J. Cell Biol.*, **45**, 355 (1970).
[32] Gilula, N. B., and P. Satir, *J. Ultrastruct. Res.*, **30**, 249 (1970).
[33] Compare with Locke, M., *J. Cell Biol.*, **25**, 160 (1965).
[34] Danilova, L. V., K. D. Rokhlenko, and A. V. Bodryagina, *Z. Zellforsch.*, **100**, 101 (1969).
[35] Goodenough, D. A., and J. P. Revel, *J. Cell Biol.*, **45**, 272 (1970).
[36] Compare with MacRae, E. K., *Z. Zellforsch.*, **82**, 479 (1967).